Short communication

Effect of titanium substitution in layered LiNiO$_2$ cathode material prepared by molten-salt synthesis

Hyung-Wook Ha, Kyung Hee Jeong, Keon Kim[*]

Division of Chemistry and Molecular Engineering, Korea University, Seoul 136-701, South Korea

Abstract

LiNi$_{1-x}$Ti$_x$O$_2$ ($0 \leq x \leq 0.1$) compounds have been synthesized by a direct molten-salt method that uses a eutectic mixture of LiNO$_3$ and LiOH salts. According to X-ray diffraction analysis, these materials have a well-developed layered structure (R3-m) and are an isostructure of LiNiO$_2$. The LiNi$_{1-x}$Ti$_x$O$_2$ ($0 \leq x \leq 0.1$) compounds have average particle sizes of 1–5 μm depending on the amount of Ti salt. Charge–discharge tests show that a LiNi$_{1-x}$Ti$_x$O$_2$ ($0 \leq x \leq 0.1$) cathode prepared at 700 °C has an initial discharge capacity as high as 171 mA h g^{-1} and excellent capacity retention in the range 4.3–2.8 V at a current density of 0.2 mA cm^{-2}.
© 2006 Elsevier B.V. All rights reserved.

Keywords: Molten-salt synthesis; Lithium battery; Lithium nickel oxide; Cycling performance; Titanium substitution; Cathode material

1. Introduction

One of the most important power sources is the rechargeable lithium-ion battery. The compound LiCoO$_2$ is an excellent positive electrode (cathode) material with good reversibility and rate capability, but it suffers from high cost and cobalt is toxic. Therefore, much effort has been made to develop cheaper and more environmentally friendly cathode materials than LiCoO$_2$. In recent years, layered LiNiO$_2$ has been studied extensively [1,2] as a possible alternative to LiCoO$_2$ because of its low cost and a large theoretical capacity (275 mA h g^{-1}).

Stoichiometric LiNiO$_2$ is known to be difficult to synthesize and its multi-phase reactions during electrochemical cycling lead to structural degradation [3]. During the charge process, LiNiO$_2$ undergoes a sequential change in crystal structure from the hexagonal phase to the monoclinic phase, to the hexagonal phase again, then two hexagonal phases, and finally a single hexagonal phase [4]. There is also concern over the thermal stability of LiNiO$_2$ in the charged state. To overcome the difficulties of synthesis and structural instability during cycling and to improve the thermal safety, the nickel ion has been substituted by various metal ions (e.g., Mg, Al, Mn, Ga) [5–8]. It has been reported that the substitution process stabilizes the crystal structure of the material during the intercalation/deintercalation of lithium ions, even in an overcharged state, and there by improves LiNiO$_2$ cycleability.

A molten-salt method has been found to be a simple means to prepare pure and stoichiometric powders of multi-component oxides, in which the molten salts are utilized as solvent or reacting species [9,10]. Since the diffusion rates of the components in molten salts are much higher than those in a solid-state reaction, the various powders, such as LiCoO$_2$, can be prepared at significantly lower temperatures [11]. Han et al. [11,12] have investigated the preparation of LiCoO$_2$ and LiCo$_{0.8}$M$_{0.2}$O$_2$ (M = Al, Ni) by molten-salt synthesis.

In this study, stochimetric LiNi$_{1-x}$Ti$_x$O$_2$ ($0 \leq x \leq 0.1$) powders are prepared by direct molten-salt synthesis using eutectic mixtures of LiNO$_3$ and LiOH molten salts. The effect of titanium on the structure and electrochemical properties of LiNi$_{1-x}$Ti$_x$O$_2$ ($0 \leq x \leq 0.1$) compounds has been investigated.

2. Experimental

LiNi$_{1-x}$Ti$_x$O$_2$ ($0 \leq x \leq 0.1$) was prepared by direct molten-salt synthesis using appropriate amounts of Ni(OH)$_2$ and (NH$_4$)$_2$TiO(C$_2$O$_4$)$_2$·H$_2$O. A 0.59LiNO$_3$–0.41LiOH flux was used as the lithium salt and had a melting point of 183 °C. A

* Corresponding author. Tel.: +82 2 953 1172; fax: +82 2 953 1172.
E-mail address: kkim@korea.ac.kr (K. Kim).

stoichiometric ratio of $Ni(OH)_2$, $(NH_4)_2TiO(C_2O_4)_2 \cdot H_2O$ and a large excess of $0.59LiNO_3$–$0.41LiOH$ flux was prepared; the molar ratios for the metal salts were 1, 5 and 10, respectively. The Ni–Ti ions to Li-salt flux molar ratio is defined here as F. The mixture was heated at 600–800 °C under an oxygen atmosphere for 30 h. The heating rate was fixed at 200 °C h^{-1} for all the temperature settings. After the heating, the resulting powders were cooled to ambient temperature and the residual fluxes were removed by washing with distilled water and 1 M acetic acid solution for 30 min. Finally, the powders were dried at 120 °C for 12 h.

To investigate the crystal structure, the prepared powders were characterized by X-ray diffraction using a Rigaku DMAX-IIIA diffractometer equipped with a Cu target. The scan data were collected in the 2θ range of 15–90°. The step size was 0.020° with a counting time of 0.4 s. Rietveld refinement [13] was performed on the X-ray diffraction profiles to confirm the crystal structure. The peak shape was described by a pseudo-Voigt function. The background level was defined by a polynomial function.

The valence states of the transition metal ions were investigated by X-ray photoelectron spectroscopy (XPS). The XPS spectra were obtained by means of a PHI (Physical Electronics) 5800 spectrometer with an Al Kα X-ray source (1486.6 eV).

The electrochemical properties of the powders were examined by using a two-electrode electrochemical cell. The cathodes were prepared by mixing 20 mg of each $LiNi_{1-x}Ti_xO_2$ ($x = 0$, 0.025, 0.05, 0.1) compound with 12 mg of conductive binder (8 mg of Teflonized acetylene black and 4 mg of graphite), pressing the resulting mixture between two aluminum plates, and then vacuum drying overnight at 120 °C. Lithium metal and a polypropylene film served as the anode and the separator, respectively. The electrolyte was 1 M $LiPF_6$ in 1:1 mixture by volume of ethylene carbonate/dimethyl carbonate (EC/DMC). The entire cell was assembled in a glove box. The electrochemical performances of the various compounds were evaluated by cycling in the 2.8–4.3 V (versus Li/Li$^+$) range at a current density of 0.2 mA cm^{-2} at room temperature.

Differential scanning calorimetry (DSC) experiments were conducted on $LiNiO_2$ and $LiNi_{0.9}Ti_{0.1}O_2$ samples charged to 4.5 V for 24 h. The data were acquired at a scan rate of 10 °C min^{-1} in the temperature range of 50–400 °C.

3. Results and discussion

The effect of calcination temperature on the formation of $LiNi_{0.95}Ti_{0.05}O_2$ is investigated. The XRD patterns recorded for $LiNi_{0.95}Ti_{0.05}O_2$ calcined at different temperatures for 30 h using the same amount of $LiNO_3$–LiOH flux, i.e., $F = 10$, are shown in Fig. 1. The material calcined at 600 °C shows very broad peaks, which indicates low crystallinity. Although all the peaks are indexable in the hexagonal lattice, calcination at 600 °C is not sufficient to impart any hexagonal lattice ordering of the lattice. Increasing the calcination temperature to 700 °C results in very sharp diffraction peaks. This suggests, complete hexagonal lattice ordering. Further increase of the calcination temperature to 800 °C causes a clear split of the (0 0 6) and
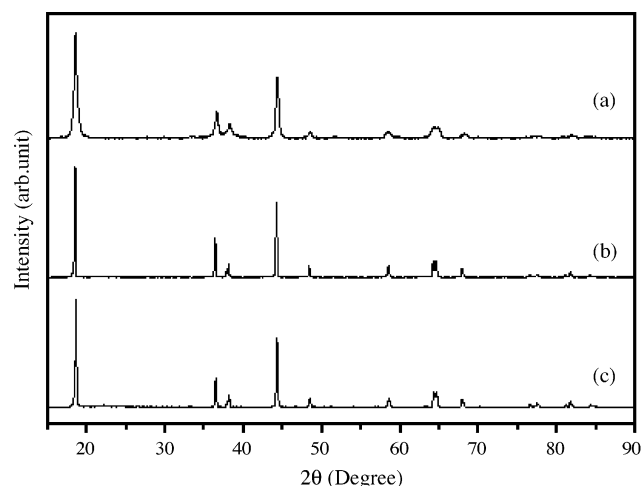

Fig. 1. X-ray powder diffraction patterns of $LiNi_{0.95}Ti_{0.05}O_2$ powders synthesized at various temperatures for 30 h in $F = 10$ system: (a) 600 °C; (b) 700 °C; and (c) 800 °C.

(1 0 2) peaks and good symmetry of the (1 0 8) and (1 1 0) peaks. Although there is very little difference between the samples calcined at 700 and 800 °C, the lower calcination temperature is more advantageous. From these results, the optimum calcination temperature is taken as 700 °C.

The effect of flux ratio, F, on the formation of $LiNi_{0.95}Ti_{0.05}O_2$ was studied for calcination at 700 °C for 30 h. The XRD patterns of the powders prepared using different F-values that range from 1 to 10 are presented in Fig. 2. Single-phase $LiNi_{0.95}Ti_{0.05}O_2$ powders were obtained under two conditions, $F = 5$, 10. Scanning electron images of $LiNi_{0.95}Ti_{0.05}O_2$ powders prepared using different amounts of $LiOH$–$LiNO_3$ are shown in Fig. 3. As the amount of $LiOH$–$LiNO_3$ salt increases, the average particle size becomes smaller and the distribution of particle size becomes narrower. It seems that the presence of a large quantity of molten-salt phase probably aids the formation of the $LiNi_{1-x}Ti_xO_2$ phase and hinders particle growth. Therefore, further studies were conducted on the $F = 10$ system.
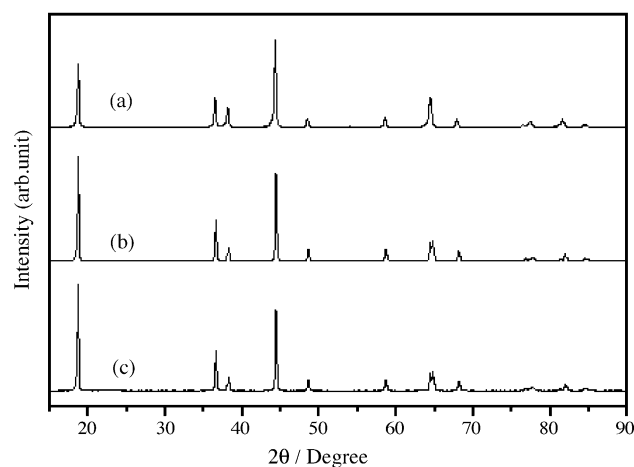

Fig. 2. X-ray powder diffraction patterns of $LiNi_{0.95}Ti_{0.05}O_2$ powders synthesized using different amounts of molten-salt flux at 700 °C for 30 h: (a) $F = 1$ (solid-state reaction); (b) $F = 5$; and (c) $F = 10$.
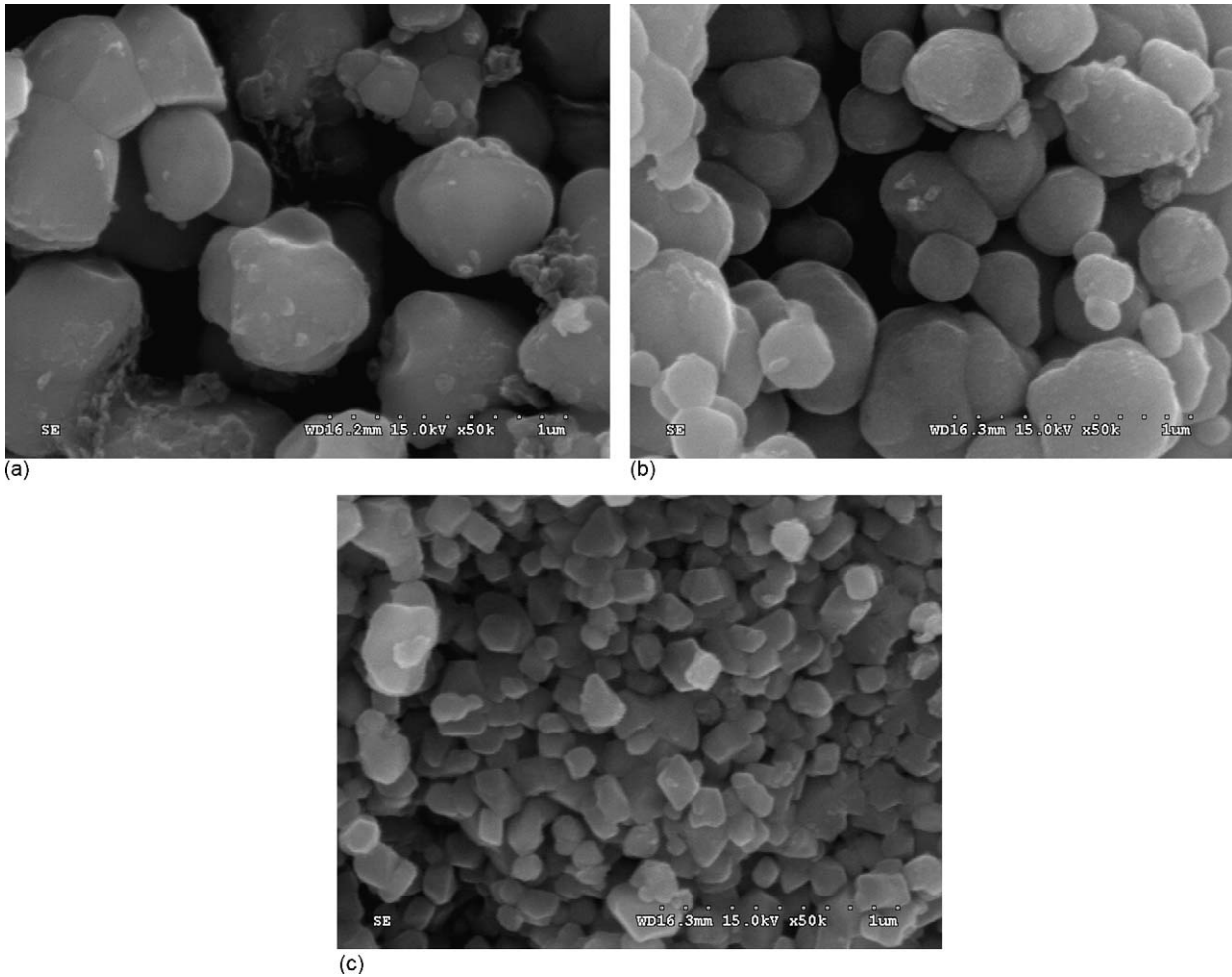
Fig. 3. Scanning electron micrographs of $LiNi_{0.95}Ti_{0.05}O_2$ powders calcined at 700 °C for 30 h using various molten-salt flux: (a) $F = 1$; (b) $F = 5$; and (c) $F = 10$.

The XRD patterns of $LiNi_{1-x}Ti_xO_2$ powders synthesized at 700 °C for 30 h using the same amount of molten salt as $F = 10$ are shown in Fig. 4. The XRD lines are quite narrow for all of the samples, which indicates quite good crystallinity of the materi-
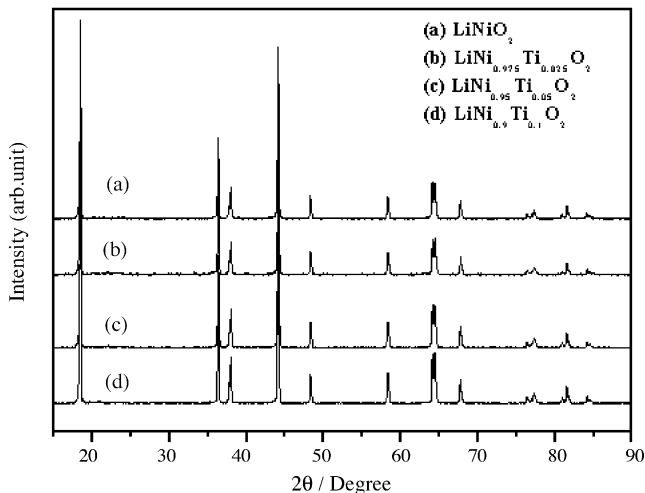

Fig. 4. X-ray powder diffraction patterns of $LiNi_{1-x}Ti_xO_2$ samples.

als. The intensity ratio of the (0 0 3) peak to the (1 0 4) peak has a relatively high value of 1.3–1.5. The ratio is generally used to examine the crystallinity of the $LiNiO_2$ phase [14]. The pattern also shows a clear split of the (0 0 6) and (1 0 2) peaks and a good symmetry of the (1 0 8) and (1 1 0) peaks. According to XRD analysis, the $LiNi_{1-x}Ti_xO_2$ ($x = 0$, 0.025, 0.05, 0.1) compounds are found to be isostructural with $LiNiO_2$, which has the rhombohedral layered structure ($R3–m$). As the titanium content increases, all of the peaks shift slightly towards lower diffraction angles because of the titanium ions substituted in the nickel sites [4].

The Rietveld refinement gave factors and the structural parameters that were in good agreement with those obtained by Croguennec et al. [15]. Increase in the a and c parameters with increasing amount of Ti ion is observed. This is because of the larger size of the titanium ions ($Ti^{4+} = 0.605$) compared with the Ni^{3+} ions ($r = 0.56$). The lattice constants a and c, as well as the c/a, $[I_{006} + I_{102}]/I_{101}$ and $I_{(003)}/I_{(104)}$ ratios are summarized in Table 1. The R-factor, which was defined by Reimers et al. [16] as $[I_{006} + I_{102}]/I_{101}$, should be at a minimum in a system with good hexagonal ordering.

From XPS analysis, the valence states of the Ti and Ni ions are found to be Ti^{4+} and Ni^{3+} and a small amount of divalent
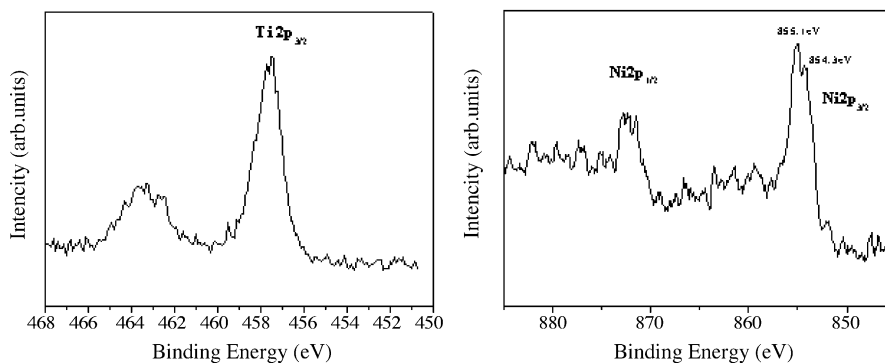
Fig. 5. XPS data of $LiNi_{0.95}Ti_{0.05}O_2$ sample.

nickel ion is detected, as shown in Fig. 5. Ti $2p_{3/2}$ lines with binding energy (BE) of 457.5 eV correspond to Ti(IV). The major Ni $2p_{3/2}$ line with a binding energy of 855.1 eV and a shoulder with a binding energy of 854.3 eV correspond to Ni^{3+} and Ni^{2+}, respectively. The tetravalent titanium ions substitute for trivalent nickel ions in $LiNiO_2$ and induce the presence of an equal amount of Ni^{2+} ions for charge compensation. The existence of

divalent nickel ions in $LiNiO_2$ causes the formation of lithium oxide impurities, and results in the presence of nickel ions in the lithium layer (3b site), that hinder the smooth transport of lithium ions through the lithium plane.

Scanning electron micrographs of $LiNi_{1-x}Ti_xO_2$ powders prepared at 700 °C for 30 h are presented in Fig. 6. Obviously, morphological changes occur as the amount of Ti increases. The
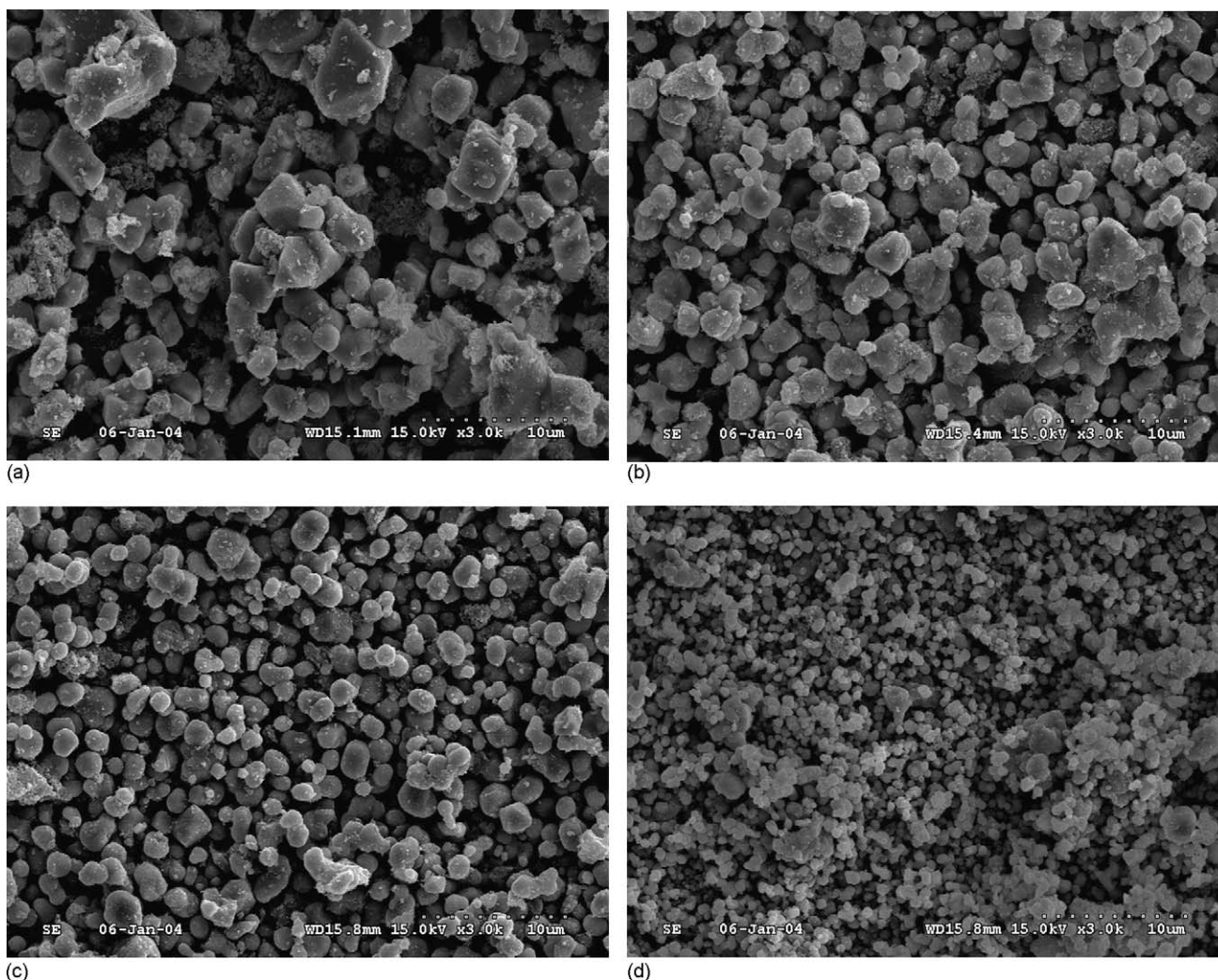

Fig. 6. Scanning electron micrographs of $LiNi_{1-x}Ti_xO_2$ samples (a) $x = 0$; (b) $x = 0.025$; (c) $x = 0.05$; and (d) $x = 0.1$.

Table 1
Lattice parameters, structural parameters of $LiNi_{1-x}Ti_xO_2$ ($x = 0$, 0.025, 0.05, 0.1)

Composition	a_{hex} (Å)	c_{hex} (Å)	c/a	$[I_{006} + I_{102}]/I_{101}$	I_{003}/I_{104}
$LiNiO_2$	2.874	14.187	4.936	0.53	1.452
$LiNi_{0.975}Ti_{0.025}O_2$	2.876	14.213	4.942	0.53	1.323
$LiNi_{0.95}Ti_{0.05}O_2$	2.885	14.239	4.935	0.55	1.232
$LiNi_{0.9}Ti_{0.1}O_2$	2.891	14.256	4.931	0.45	1.153

$LiNiO_2$ powders are smooth-edged polyhedral and their average size is approximately 3–5 μm. The $LiNi_{1-x}Ti_xO_2$ ($x = 0.1$) sample, however, has close to spherical morphology and an average particle size of less than 1 μm. As the amount of Ti increases, the average particle size becomes smaller and the distribution of particle size becomes narrow.

Charge–discharge curves between 2.8 and 4.3 V at a constant current density of 0.2 mA cm^{-2} are presented in Fig. 7 for $LiNi_{1-x}Ti_xO_2$ cathodes. The $LiNi_{0.975}Ti_{0.025}O_2$ sample has an initial capacity of 171 mA h g^{-1} and a value of 164 mA h g^{-1} on the 30th cycle. Thus, the material displays remarkable capacity retention. The electrochemical performance of $LiNi_{1-x}Ti_xO_2$ is superior, or comparable with that of the $LiNiO_2$ system. Since Ti^{4+} is not electrochemically active in the voltage range of 4.3–2.8 V, the capacity decreases almost linearly as the titanium increases. The existence of divalent nickel ions in the $LiNiO_2$ system may be responsible for the poor capacity and irreversible capacity loss of the $LiNiO_2$ system. In fact, good electrochemical performance of $LiNi_{1-x}Ti_xO_2$ ($x = 0$, 0.025, 0.05, 0.1) is achieved by preventing the migration of impurity Ni^{2+} ions into the lithium plane by substituting tetravalent titanium ions into the structure.

The results of differential scanning calorimetry tests are shown in Fig. 8. These were performed to study the thermal stability of the $LiNi_{1-x}Ti_xO_2$ materials, especially in the charged

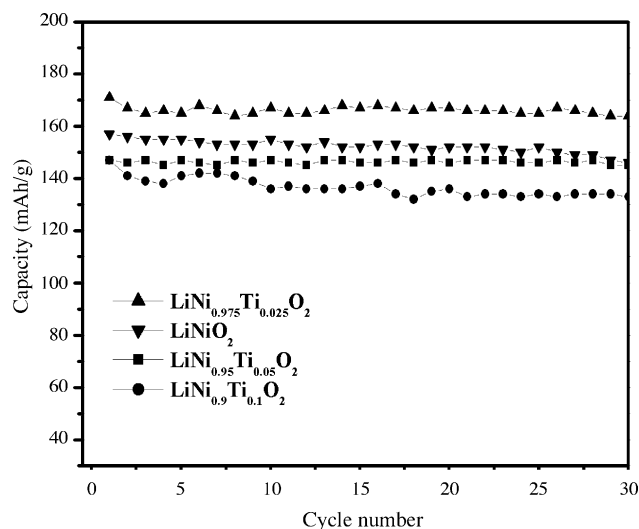Fig. 8. Differential scanning calorimetry profiles (10 °C min^{-1}) of (a) $LiNiO_2$; and (b) $LiNi_{0.9}Ti_{0.1}O_2$ charged at 4.5 V for 24 h.

state. The DSC profile of $LiNiO_2$ charged to 4.5 V has a sharp exothermic peak at about 220 °C. This peak is obviously of great safety concern for Li-ion batteries using $LiNiO_2$ as the cathode material [17]. As shown in Fig. 8(b), $LiNi_{0.9}Ti_{0.1}O_2$ material has much smaller exothermic reaction at about 230 °C. This indicates that $LiNi_{0.9}Ti_{0.1}O_2$ has better thermal safety characteristics than $LiNiO_2$.

4. Conclusions

$LiNi_{1-x}Ti_xO_2$ ($0 \leq x \leq 0.1$) powders are synthesized as an alternative cathode material for lithium batteries by a direct molten-salt method using a eutectic mixture of $LiNO_3$ and LiOH salts. The valency states of the transition metals are Ti(IV) and Ni(III), as determined by XPS studies. The particles of the $LiNi_{1-x}Ti_xO_2$ ($0 \leq x \leq 0.1$) powders have spherical morphology. A $LiNi_{0.975}Ti_{0.025}O_2$ cathode exhibits an initial discharge capacity of 171 mA h g^{-1} and an excellent capacity retention over 30 cycles. Its electrochemical performance is superior to that of the $LiNiO_2$ system. Differential scanning calorimetry experiments revealed that $LiNi_{0.9}Ti_{0.1}O_2$ has better thermal stability than $LiNiO_2$ cathode material.

Fig. 7. Evolution of charge and discharge capacities with number of cycles of $LiNi_{1-x}Ti_xO_2$ ($x = 0$, 0.025, 0.05, 0.1) cells at current density of 0.2 mA cm^{-2} between 2.8 and 4.3 V.

References

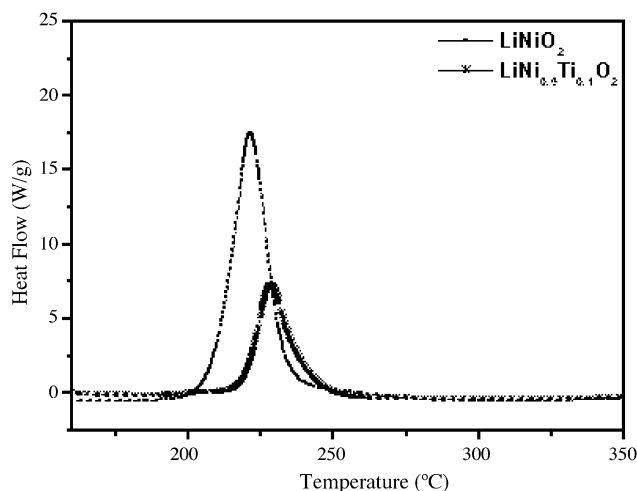[1] J.R. Dahn, U. Sacken, M.W. Juzkow, H. AI-Janaby, J. Electrochem. Soc. 138 (1991) 2207.
[2] W. Ebner, D. Fouchard, L. Xie, Solid State Ionics 69 (1994) 238.
[3] M.E. Arroyo y de Dompablo, G. Ceder, J. Power Sources 119–121 (2003) 654.
[4] T. Ohzuku, A. Ueda, M. Nagayama, J. Electrochem. Soc. 140 (1993) 1862.

[5] B.V.R. Chowdari, G.V. Subba Rao, S.Y. Chow, Solid State Ionics 140 (2001) 55.

[6] S.H. Park, K.S. Park, Y.K. Sun, K.S. Nahm, Y.S. Lee, M. Yoshio, Electrochim. Acta 46 (2001) 1215.

[7] Y. Makimura, T. Ohzuku, J. Power Sources 119–121 (2003) 156.

[8] Y. Nishida, K. Nakane, T. Satoh, J. Power Sources 68 (1997) 561.

[9] C.C. Chiu, C.C. Li, S.B. Desu, J. Am. Ceram. Soc. 74 (1991) 38.

[10] K.H. Yoon, Y.-S. Cho, D.-H. Lee, D.-H. Kang, J. Am. Ceram. Soc. 76 (1993) 1373.

[11] C.H. Han, Y.S. Hong, C.M. Park, K. Kim, J. Power Sources 92 (2001) 95.

[12] C.H. Han, Y.S. Hong, K. Kim, Solid State Ionics 159 (2003) 241.

[13] J. Rodriguez-Carvajal, Program Fullprof, Version 3.2, LLB JRC, January, 1997.

[14] M.Y. Song, R. Lee, J. Power Sources 111 (2002) 97.

[15] L. Croguennec, E. Suard, P. Willmann, C. Delmas, Chem. Mater. 14 (2002) 2149.

[16] J.N. Reimers, E. Rossen, C.D. Jones, J.R. Dahn, Solid State Ionics 61 (1993) 335.

[17] Y. Gao, M.V. Yakovleva, W.B. Ebner, Electrochem. Solid State Lett. 1 (1998) 117.